Comparative Life Cycle Assessment of Injection Molded and Big Area Additive Manufactured NdFeB Bonded Permanent Magnets

Sameer Kulkarni
Mechanical Engineering,
Purdue University,
West Lafayette, IN 47907
e-mail: kulkar15@purdue.edu

Fu Zhao[1]
Environmental and Ecological Engineering,
Purdue University,
West Lafayette, IN 47907;
Mechanical Engineering,
Purdue University,
West Lafayette, IN 47907
e-mail: fzhao@purdue.edu

Ikenna C. Nlebedim
Critical Materials Institute,
Ames Laboratory,
Ames, IA 50011
e-mail: nlebedim@ameslab.gov

Robert Fredette
USA Rare Earth,
LLC, Stillwater, OK 74075
e-mail: robert.fredette@usare.com

Mariappan Parans Paranthaman[1]
Chemical Sciences Division,
Oak Ridge National Laboratory,
Oak Ridge, TN 37831
e-mail: paranthamanm@ornl.gov

Permanent magnets are expected to play a crucial role in the realization of the clean economy. In particular, the neodymium–iron–boron ($Nd_2Fe_{14}B$ or NdFeB) magnets, which have the highest energy density among rare earth permanent magnets, are needed for building more efficient windmill generators, electric vehicle motors, etc. Currently, near-net shape magnets can be either made through sintering and compression molding with extensive post machining or directly through injection molding. However, injection molding has a loading volume fraction limitation of 0.65 for nylon binders. A novel method of manufacturing bonded permanent magnets with loading fraction greater than 0.65 has been demonstrated using big area additive manufacturing (BAAM) printers. As energy density is directly proportional to the square of the magnet loading fraction, magnets produced using BAAM printers require less volume and magnetic material compared to that of injection molded magnets on average. A comparative life cycle assessment shows that this difference in magnetic powder consumption nearly constitutes the difference in the environmental impact categories. Even after assuming recycled magnetic input, the BAAM magnets perform better environmentally than injection molded magnets, especially in the ozone depletion category. Since BAAM printers can accommodate even higher loading fractions, at scale, BAAM printers possibly can bring about a significant decrease in rare earth mineral consumption and environmental emissions. Furthermore, single screw extrusion enables BAAM printers to have high print speeds and allow them to be economically competitive against injection molding. Therefore, BAAM printed magnets show great promise in transitioning towards the clean economy. [DOI: 10.1115/1.4056489]

Keywords: NdFeB nylon bonded permanent magnets, injection molding, additive manufacturing or 3D printing, life cycle analysis, injection molding and other polymer fabrication processes, nontraditional manufacturing processes, sustainable manufacturing

1 Introduction

Magnets, often not explicitly visible, are ubiquitous in the modern world. Their applications range from large-scale industrial machines (e.g., generators in windmills) to small commercial products (e.g., toys). Since the discovery of neodymium iron boron ($Nd_2Fe_{14}B$ or NdFeB) permanent magnets in 1984, they have been the focus of research due to their vastly superior calculated maximum energy product, $(BH)_{max}$, of 512 kJ/m^3 [1]. Today, NdFeB magnets are the strongest commercially available permanent magnets and are used for a variety of products such as hard drives, household electric appliances, hybrid and electric vehicles, sensors, actuators, unmanned ariel vehicles, and wind turbines amongst other applications [2,3]. NdFeB magnets also contain a combination of various other rare earth minerals such as dysprosium, praseodymium, terbium, etc. that help add various characteristics to the final magnet (such as temperature performance, improved magnetic properties, etc.) that are needed depending on the different applications. Due to this heavy dependence on rare earth elements (REEs) for electronics and devices crucial to the transition towards a cleaner economy, it is predicted that consumption of neodymium could grow by 700% till 2027 [4]. Since the vast majority of the REE is sourced from China [5], the U.S. Department of Energy has classified these metals as critical materials (defined as heavily import reliant minerals that are vital to nation's security and economic prosperity [6]). Therefore, it is prudent to explore new manufacturing alternatives that can help reduce the reliance on these minerals.

Depending on the applications, NdFeB magnets can be manufactured in multitude of mechanisms—sintering, compression, or injection molding (IM), calendaring, etc. Sintered NdFeB magnets are aligned, compacted, and heated to 1000–1100 °C [7] to achieve high density and are the strongest of the NdFeB magnets. However, due to the poor mechanical strength, these magnets are incredibly brittle and can only be made into simple geometrical shapes. Compression molding requires mixing the magnet powder with epoxy or resin-based polymer binders (up to 80% magnet powder and 20% polymer by volume), heating these powders to slightly elevated temperatures, and pressing them into a mold at high pressures. Once again, these magnets can only be typically made into simple geometrical shapes. Therefore, both sintering and compression molded magnets typically require extensive post manufacturing processing to meet the geometric requirements for the final application. Injection molded magnets utilize pellets

[1]Corresponding authors.

Manuscript received August 23, 2022; final manuscript received December 13, 2022; published online January 19, 2023. Assoc. Editor: Sara Behdad.

composed of mixture of magnetic and thermoplastic polymer binders to produce near-net shape magnets at relatively large scales. Calendaring also feeds in a polymer–magnet mixture that is fed through rolling processes to generate long flexible magnetic sheets (these processes along with others are discussed in depth in Refs. [8,9]). Magnets utilizing a polymer matrix (i.e., compression molding, injection molding, or calendaring) are known as bonded magnets. These magnets are not as dense as sintered magnets, resulting in lower magnetic strength. Bonded magnets have a wide range of demand—hard drives, home appliances, consumer electronics, generic motors, or sensors [10]. Sintered magnets are typically reserved for applications requiring high strength magnetic performance, such as generators or high-performance motors. These sintered magnets are also typically pricier and have a higher weight (due to being 100% magnetic material compared to magnet–polymer mixture for bonded magnets). The high material costs and weight combined with a radical increase in demand for large generators (windmill generators), there is increasing interest in magnets with lower energy products for these large applications [11].

Recently, a novel way to manufacture rare earth permanent magnets via additive manufacturing was proposed. This method successfully printed bonded neodymium magnets [12–14] and was made possible due to big area additive manufacturing (BAAM) 3D printer. Unlike a conventional nozzle-based fused deposition modeling (FDM) printer with a filament feedstock, BAAM utilizes a single screw extruder and composite pellet feedstocks (similar to extruded pellets used for injection molding). The use of single screw allows for viscous heating and gets rid of the requirement of needing an oven (the heated printed area typically present in FDM printers), making it easier for the printer to scale and consume less energy. Therefore, BAAM printer allows for a significantly larger printing workspace than the average fused deposition modeling printer, with dimensions of $240'' \times 90'' \times 72''$. It can also print at fast speeds of up to 80 lb/h, making it comparable to other large-scale manufacturing methods [15] like injection molding. Furthermore, magnets produced through this method have properties better than or comparable to injection molded magnets [12]. Both manufacturing methods produce near-net shape magnets and have comparable mechanical (such as Young's modulus or ultimate strength) properties. While injection molding technique requires a mold for fabricating parts, 3D printing achieves near-net shape manufacturing via layer-by-layer printing. Furthermore, it has been shown that the resolution of BAAM printing can be improved by reducing extruder diameter through the use of a poppet within the deposition nozzle during printing the exterior layer to produce smaller layer sizes and more precise contouring of the final shape [16].

As mentioned before, rare earth magnets are expected to play a pivotal role in the transition towards a so called "net zero economy." It is important, therefore, to ensure that the magnets used in these environmentally conscious technologies such as generators for windmills or motors for electric vehicles are themselves produced in an environmentally responsible manner. Life cycle assessment (LCA) is a widely accepted methodology used to assess environmental impacts of products or processes. Particularly, a comparative LCA allows for the contrasting between substitutable products or process to determine which product or process has the least damage on the environment. Previous permanent magnet LCA studies have mostly looked at conducting LCAs for sintered NdFeB magnets [17] and built a comprehensive inventory for rare earth metal mining, processing, and the sintering of the raw material into the magnet. Sprecher et al. [17] also considered differences in recycled and primary neodymium metal inputs and found orders of magnitudes of improvement for recycled metal. Jin et al. looked at virgin versus recycled sintered NdFeB magnet production and found similar results [18]. Langkau and Erdmann conducted an LCA for producing 1 kg of common rare earth minerals used in permanent magnets and projects environmental impact in the future (till 2035) factoring demand, supply, and policy measures [19]. This study concludes that lowering demand (by improving material efficiency) results in the lowest environmental impact in the future. Arshi et al. build a complete location and mine-based life cycle inventory (LCI) and calculate environmental impacts for common rare earth products such as sintered permanent magnets and phosphors [20]. As can be seen, no studies regarding injection molded or additively manufactured bonded permanent magnets were found. In this research, due to their alike use cases, a comparative LCA is conducted to determine the environmental impacts of novel additive manufacturing methods compared to that of injection molding. An LCA conducted early in a technology's growth can help guide its development and help make its eventual wide-scaled implementation more sustainable.

2 Methodology

The cradle to gate comparative life cycle assessment was performed following the four steps (goal and scope definition, LCI for both injection molded and BAAM magnets, life cycle impact assessment, and interpretation) stated in ISO 14040 standard [21].

2.1 Goal and Scope Definition. The goal of this LCA is to evaluate the environmental impacts between two processes for manufacturing of magnets—IM and additively manufacturing (AM). However, assessing various other magnet manufacturing techniques can be a difficult task due to the lack of a clear basis of comparison. Magnets have many diverse applications that each have different desired or required characteristics such as final geometry (near-net shape) requirement, thermal resistance, mechanical properties, hysteresis, demagnetization resistance, corrosion resistance, etc. [22]. Therefore, selecting a functional unit becomes a challenging task, especially when the eventual application of the magnet is not known. For comparison between AM and IM methods, the maximum energy product—$(BH)_{max}$—is chosen as the basis for the functional unit for this LCA, as this property can be a general representation of the strength of a magnet and is often used as a representation of a magnet's grade [23]. Since $(BH)_{max}$ is volume dependent, the product of a hypothetical volume of 0.0001 m^3 and energy product of 50 kJ/m^3 is set as the functional unit (0.005 kJ) requirement for the IM and AM magnets to match (to allow for IM and AM magnets to have different volumes, as is the case in reality). This can be accepted as a sensible function unit as it has basis in practical application. It has been shown that the torque generated by a permanent magnet motor is proportional to the product of magnet $(BH)_{max}$, magnet volume, and the quadric root of the diameter of the motor rotor [24]. Therefore, for a constant torque requirement, the motor that contains the magnet with the higher energy product will require a lower magnet volume. This functional unit choice now enables us to account for differences in magnetic strength of the IM and AM magnets. It is assumed that the impact of geometry of the magnets on the energy product is similar between injection molded and additively manufactured magnets.

As mentioned above, the scope of the LCA is cradle to gate. Infrastructure and transportation are not considered as they are either assumed to be negligible or similar between the two manufacturing processes. This includes the single screw extruder used by both manufacturing techniques, as this can be considered consumable and requires replacement. As the AM magnets have higher loading fraction, it can be expected that the single screw extruder will be consumed at higher rates for AM compared to IM. However, it is assumed that the inclusion of this within the system boundary on a per functional unit basis is negligible and therefore not considered. One exception is made in the inclusion of infrastructure, which is the coating of the mold. That is because the mold (or tooling) gets coated periodically (since the mold manufacturing process can be highly expensive and time consuming, it is cheaper to coat the molds periodically than remaking the mold) to better handle the abrasive nature of the feedstock. These coating materials can have a high environmental impact and are therefore included in the scope. Similar such coating

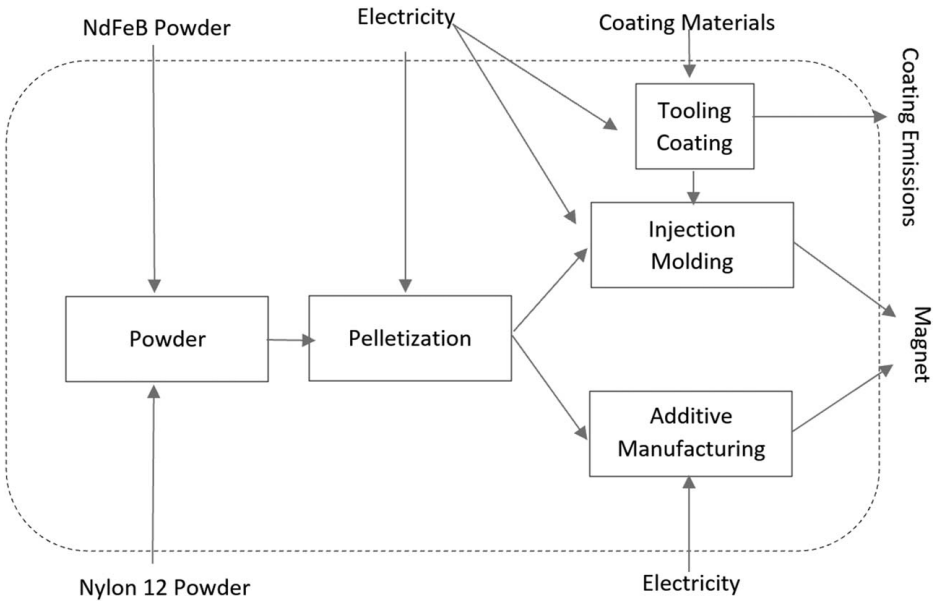

Fig. 1 System boundary for comparative LCA (transportation and infrastructure not considered)

Table 1 AM and IM magnet properties ($(BH)_{max}$ values sourced from Ref. [12])

	Magnet properties				
Types of magnet	Max energy product (kJ/m^3)	Magnet volume needed (m^3)	Magnet mass (kg)	Magnet powder needed (kg)	Polymer powder needed (kg)
IM magnet	36.17	0.000138	0.738	0.683	0.0552
AM magnet	43.49	0.000115	0.651	0.612	0.0393

Note: Mass and volume values for magnets calculHted based on the functional unit of 0.005 kJ/m^3 and $(BH)_{max}$.

(outside of the single screw extruders, which are not included in the scope for reasons explained above) is not required for tools used in 3D printing. Furthermore, potential eventual alignment of the magnet (for anisotropic magnets) is not included within the scope. The overarching system boundary is shown in Fig. 1—note that this includes the preparation of the extruded magnet–polymer pellets, which is not assumed to be similar between IM and AM due to reasons discussed below. It is assumed that the reject rate for both IM and AM techniques is similar (mostly due to the ease in reusing reject as feed stock) and therefore not considered.

2.2 Life Cycle Inventory. Before calculating inventories for the two manufacturing pathways, it is important to distinguish a key difference in the highest loading fraction (f) possible for AM and IM magnets. The loading fraction is the percentage by volume of the magnetic material in magnet–polymer composite powder. Traditional IM magnets have been limited to a loading fraction of 65%. This is because IM requires a minimum amount of binder/polymer within the mixture to maintain appropriate fluid viscosity for the plastic flow to appropriately fill out the mold [10]. It has been shown that the loading fraction for the IM process can be increased to 70% using spheroidized magnetic powder [25]. However, while spheroidal particles lower viscosity (allowing for the higher loading fraction), the resulting magnets are isotropic and have a low magnetic performance. Furthermore, magnets with spheroidal morphology have been shown to have a weaker mechanical strength compared to flake morphology magnets [26]. Hence, typically IM magnets are limited to a loading fraction of 65%. Previous work shows that BAAM printed magnets can accept $f \geq 70\%$ without requiring spheroidized magnetic powder [27]. This distinction is crucial as the energy product is directly proportional to the square of f [28]. Therefore, AM magnets, on average, have a higher possible (BH_{max}) than IM magnets. Table 1 shows the magnetic and physical properties for both IM and AM magnets. The polymer chosen as the bonding material is Nylon 6.

The necessary magnet volume (in relation to the functional unit) is calculated using (1). Then using the volume, f, and the magnet and Nylon 6 density, the mass for magnet and polymer powders can be calculated (for both AM and IM magnets).

$$V_{\text{magnet}} = \frac{50\ \frac{\text{kJ}}{\text{m}^3} * 0.0001\ \text{m}^3}{(\text{BH})_{\text{max,maget}}} \tag{1}$$

$$m_{\text{magnet}} = V_{\text{magnet}} f \rho_{\text{magnet}} \tag{2}$$

$$m_{\text{polymer}} = V_{\text{magnet}}(1-f)\rho_{\text{polymer}} \tag{3}$$

The theoretical densities assumed for the NdFeB and the Nylon 6 powder were 7.6 g/cm^3 [12] and 1.14 g/cm^3 [29], respectively. As can be seen in Table 1, quantity and the composition of the magnet–polymer powder are different for IM and AM magnets, resulting in slightly different feedstocks for the two manufacturing pathways. Due to this difference, the extrusion process to make pellets cannot be assumed to be similar across IM and AM magnets and must be included.

2.2.1 Powder. Table 1 already describes the amount of magnetic and polymer powder needed for IM and AM magnets. For the magnetic powder, the inventory data are sourced from the excel tool provided by Ref. [20] with few modifications to the sintered magnet inventory—the electricity is scaled by 75% (assuming

Table 2 LCI for injection molded magnets—powders

Materials	Amount	Unit	Source
NdFeB powder	0.683	kg	CMLCAT [20]
Nylon 6	0.0552	kg	Ecoinvent—Nylon 6-6 {RoW}|market

the 25% goes towards sintering and compression) [18], the nitrogen consumption is neglected, TDK process is used, and the Nd is sourced from Bastnasite/Monazite mixture. Lastly, the inventory data for Nylon 6 is approximated by the Nylon 6,6 inventory data sourced from EcoInvent [30] (Tables 2 and 3).

2.2.2 Extrusion Process to Make Pellets. The pellets used in injection molding and BAAM printing are made by inserting a blended mixture of magnet and polymer powder at the desired loading fraction into a hopper with a powerful auger that feeds it into a twin screw compound extruder heated to around 200 °C. The extruded material is then pressed through multi-orifice die precisely at 10 kg/h with a rotating die face cutter to make uniform pellets. As a last step, the pellets are dried at 60 °C for 4 h [12] and are ready to be used in manufacturing.

Since there is a lack of experimentally measured data for the pellet making process, energy consumption calculations have to be estimated for an industrial scale. Piccinno et al. provide a scale-up framework from laboratory to industrial scale of common chemical processes for various batch sizes. Using this framework, the energy consumption for blending of the magnetic and polymer powders is modeled as rotor stator homogenizing stirring/mixing in Eq. (4), where N_p is the power number of the impeller, d is the diameter of the impeller, N is the rotational speed of the agitator, η_{stir} is the efficiency of the agitator, and t is the amount of time the mixture is stirred. The values for the different parameters are taken from Ref. [31] at the 1000 m^3 (liter) scale (assuming that a large batch is blended at the same time) and the amount of time assumed to be 3600 s (a conservative assumption to ensure the final mixture has a homogenous blend to ensure consistent quality in the pellets).

$$E_{\text{stir}}(\text{J}) = \frac{N_p \rho_{\text{mix}} N^3 d^5 t}{\eta_{\text{stir}}} = \frac{2.39\ \rho_{\text{mix}} (48.333)^3 (0.139)^5 t}{0.9} \tag{4}$$

Both the extrusion (which is essentially the heating of powder mixture) and drying steps are modeled using the equation and scaled parameters for heating energy at the 0.1 m^3 scale shown in Eq. (5). The time for extrusion is estimated from the scale and the feed rate is 10 kg/h, the room temperature is assumed to be 25 °C, and the rest of the parameters are taken from Ref. [31].

$$Q_{\text{react}} = \frac{(c_{p,\text{polymer}} m_{\text{polymer}} + c_{p,\text{magnet}} m_{\text{maget}})(T_r - T_0) + (A k_a / s)(T_r - T_{\text{out}})t}{\eta_{\text{heat}}} \tag{5}$$

Note that there exist several models for calculating power consumption of twin screw extrusion [32,33]. However, data regarding rated power for the motor, along with torque %, the screw speed, etc was not unavailable for the pelletization process, making it difficult to calculate power consumption. However, Liang et al. [32] show that the efficiency for twin screw extruder is below 50% and that the power consumption is proportional to the viscosity of the solid flow and the melt flow while the magnet–polymer mixture travels through the extruder. Therefore, for the melting energy, η_{heat} is assumed to be 50%, and pelletization energy for additive manufacturing is multiplied by a factor of 1.1 to account for higher viscosity encountered by the extruder due to the higher loading fraction. No such factor is used for the drying energy. The efficiency specified in Ref. [31] is also used for the drying energy instead. The calculated energy consumption values for the pelletizing process at the industrial scale are then sized accordingly to the volumes of AM and IM magnets (set according to the functional unit) and are shown in Tables 4 and 5.

Table 3 LCI for additively manufactured magnet—powder

Materials	Amount	Unit	Source
NdFeB powder	0.612	kg	CMLCAT
Nylon 6	0.0393	kg	Ecoinvent—Nylon 6-6 {RoW}|market

Table 4 LCI for injection molded magnet—extrusion

Unit process	Amount	Unit	Source
Mixing energy	0.0413	MJ	Electricity, at grid, SERC, 2010/kWh/RNA
Heating energy	0.2023	MJ	Electricity, at grid, SERC, 2010/kWh/RNA
Drying energy	0.0783	MJ	Electricity, at grid, SERC, 2010/kWh/RNA

2.2.3 Manufacturing. Following the LCIs for preceding steps, the energy consumption for manufacturing one part was calculated for both injection molding and additive manufacturing. Although a per magnet approach is taken to calculate the energy consumption, it is assumed that both these manufacturing processes are producing the magnets at large scales. For the BAAM printer, these parts are made side by side contiguously on the same large print surface at high speeds (approximately 80 lb/h; [15]), making its manufacturing speed comparable to injection molding. For injection molding, an additional consideration regarding the coating of tooling is made and is discussed more in depth below.

2.2.3.1 Injection Molding. IM is a ubiquitous processing technique used to manufacture mostly plastics at large scales (size, volume, speed, etc.). A big advantage of this technique is that it allows for the production at scale of complex geometries at relatively inexpensive costs, making it a popular manufacturing technique around the world [34]. The general idea is to inject the molten feedstock into a mold cavity (tool), wait for the part to cool, separate it from the cavity, and restart the process again with the next batch. Typically, the feedstock takes forms of small pellets, which are molten through the help of a screw extruder (which utilizes viscous heating generated from the high friction created when the screw pushes the pellets against the screw chamber) and supplementary heaters. After the "injection" of the

Table 5 LCI for additively manufactured magnet—extrusion

Unit process	Amount	Unit	Source
Mixing energy	0.0365	MJ	Electricity, at grid, SERC, 2010/kWh/RNA
Heating energy	0.1921	MJ	Electricity, at grid, SERC, 2010/kWh/RNA
Drying energy	0.0669	MJ	Electricity, at grid, SERC, 2010/kWh/RNA

feedstock into the mold, the tool is clamped at high pressure to help obtain the final geometry and then allowed to cool to be removed. Metal injection molding is very similar to plastic IM. Here, there is a polymer binder that melts and uniformly holds together (assuming homogenous pellets) the metallic powder in the resulting mixture. A detailed unit process assessment done by Raoufi et al. gives the necessary equations to estimate the energy consumption per metal injection molded part [35]. The total energy consumption is the sum of basic energy (the auxiliary power used by machine to keep the systems running), injection energy (the energy needed to melt the material, inject it into the mold, and keep the cavities packed as the material shrinks), and clamping energy (which is a linear combination of cooling energy and resetting energy). The numerous equations used to calculate these energies are provided in order below (for more information on derivations and the values for the injection molding related parameters and constants, see Ref. [35]). Note that the number of cavities per mold (n_{cav}) was decided to be 4.

$$E_{melt} = [\rho_{nylon6,6} V_{nylon6,6} c_{p,nylon6,6}(T_{inj} - T_{am}) + H_{nylon6,6}] + \rho_{NdFeB} V_{NdFeB} c_{p,NdFeB}(T_{inj} - T_{am}) c_{melt} \quad (6)$$

where $H_{nylon6,6}$ is the heat of fusion for Nylon 6, set as 114.88 kJ/kg [36]. The injection molding temperature is selected to be 270 °C and the ambient temperature as 25 °C. The density and volume for the Nylon 6 and NdFeB powder are as provided in Table 1.

$$E_{mat_{inj}} = \frac{p_{inj} V_{shot}}{\eta_{screw}} \quad (7)$$

where p_{inj} is the injection pressure, V_{shot} is the shot volume (slightly larger than part volume—see Ref. [35] on how to calculate), and η_{screw} is the energy efficiency of the screw motor.

$$E_{pack} = \frac{c_2 p_{inj} V_{shot} \varepsilon}{\eta_{screw}} \quad (8)$$

where ε is the volumetric shrinkage experienced by the molded magnetic part as it is pushed into the cavities.

$$E_{injection} = \frac{E_{melt} + E_{mat_{inj}} + E_{pack}}{n_{cav}} \quad (9)$$

The melting, injection, and packing energies are all for the entire mold, so the total energy of injection per part is the sum divided by the number of cavities. To calculate the clamping energy, first we calculate the energy required to cool the part and reset the injection molding machine. The COP or coefficient of performance is representation of the effectiveness of the cooling equipment and is multiplied by η_{cool} to get the total efficiency of the cooling system. The resetting energy is estimated to be 25% of the injection, cooling, and melting energy.

$$E_{cool} = \frac{[\rho_{nylon6,6} V_{nylon6,6} c_{p,nylon6,6}(T_{inj} - T_{ej}) + H_{nylon6,6}] + \rho_{NdFeB} V_{NdFeB} c_{p,NdFeB}(T_{inj} - T_{ej})}{(COP)\,\eta_{cool}} \quad (10)$$

$$E_{reset} = 0.25 \frac{E_{mat_{inj}} + E_{cool} + E_{melt}}{\eta_{clamp}} \quad (11)$$

$$E_{clamping} = \frac{E_{cool} + E_{reset}}{n_{cav}} \quad (12)$$

Finally, a basic power consumption is also calculated. This represents the energy used to maintain the auxiliary components of the system (sensors, timers, etc.) that are not explicitly modeled.

$$E_{basic(IM)} = \frac{P_{basic(IM)} t_{basic(IM)}}{n_{cav}} \quad (13)$$

$$E_{MIM} = E_{basic(IM)} + E_{injection} + E_{clamping} \quad (14)$$

Inputting the data into Eqs. (6)–(14), we get the breakdown of the energy consumption for producing one injection molded magnet (sized according to the functional unit) as shown in Table 6.

Table 6 LCI for injection molded magnet—injection molding

Method	Unit process	Amount	Source
Injection molding (MJ)	Basic energy	0.0035	Electricity, at grid, SERC, 2010/kWh/RNA
	Injection energy	0.197	
	Clamping energy	0.144	
	Total	0.345	

A fundamental component of injection molding is its tooling (or molds). Properly designing, dimensioning, and manufacturing tooling for different geometries is a time consuming and an expensive process. The molds operate at high temperatures and pressures with abrasive feedstocks, requiring them to get periodically strengthen via coating. A commonly applied coating is titanium nitride (TiN), which provides wear and corrosion resistance along with some lubrication. Due to the high volume of parts that can be made per mold, it is assumed that the per part impact of the mold is negligible. However, since the tooling gets coated several times during its life, the coating is included within the LCA. Fiameni et al. [37] provide a detailed LCI on using physical vapor deposition to coat a small 25 cm^2 steel substrate with 3 μm of aluminum titanium nitride. This inventory is scaled linearly to 5000 cm^2 surface area (with 3 μm coating thickness) to represent the LCI for coating the mold. Assuming that the mold is coated once for every 50,000 batches (and since we have four cavities—every 200,000 parts), we can estimate the inventory on a per part basis (shown in Table 7).

2.2.3.2 Big Area Additive Manufacturing. BAAM printers are unique from other FDM printers. Traditional FDM printers utilize nozzles that require a filament feedstock, which are typically made through an energy intensive extrusion process [38]. Previous literature shows that filament-based FDM printers have an upper limit on mass flowrate dependent purely on nozzle geometry (due to heat transfer limitations). This results in a peculiar observation—larger FDM printers have a higher energy intensity (J/kg), reducing the ability of filament-based FDM printers to scale operations [15]. However, BAAM utilizes pellet-based (screw) extruders, which have a significantly higher mass flow upper limit, as it takes advantage of viscous heating along with auxiliary resistive band heating [39]. The auxiliary heating is spaced in five zones along the screw chamber, allowing for print speeds up to 11 in./s [40]. This extruder (seen in Fig. 2) is placed on a modified laser cutting four-axis gantry system that uses linear drive motors that can accelerate at 64.4 in./s^2 to peak velocities of 200 in./s [41]. A heated bed is also utilized (as opposed to a heated chamber) to help with bonding between layers. BAAM printers, by sacrificing resolution, can print at speeds and have an energy intensity comparable to injection molding [15]. This is valid for permanent magnets in which, instead of fine resolution, the magnetic performance is of interest.

Fig. 2 BAAM extruder during a print

For the LCA, the nozzle diameter and print speed were assumed to be 0.762 cm and 2.54 cm/s (although BAAM printers can print greater than 27.94 cm/s depending on the part geometry and material), resulting in a layer thickness of 0.38 cm. Using a significantly lower deposition speed also improves the resolution, as they are inversely related [16]. Therefore, it is assumed that no significant post-processing will be needed (in comparison to post-processing needed for IM magnets). The material was extruded at 255 °C onto a heated bed at 95 °C (more details regarding the printing process can be found in Ref. [28]). Therefore, the volumetric flowrate and the necessary print time can be calculated using Eqs. (15) and (16) (shown below).

$$\dot{m}_{\text{flowrate}} = v_{\text{print}} \left(\frac{\pi d^2}{4} \right) \rho_{\text{magnet}} \tag{15}$$

where $\dot{m}_{\text{flowrate}}$, v_{print}, d, and ρ_{magnet} are mass flowrate, print speed, nozzle diameter, and density of the magnet–polymer powder for the BAAM printer, respectively.

$$t_{\text{print}} = \frac{V_{\text{magnet}}}{\dot{m}_{\text{flowrate}}} \tag{16}$$

where t_{print} and V_{magnet} are the estimated print time and the required volume for the BAAM magnet, respectively. Therefore, the print time per part is estimated to be 99.25 s. Due to a lack of a reported power rating for the BAAM printer, the power rating of a similar printer, Gigabot X XLT, is used. The Gigabot X XLT also utilizes a pellet extrusion process, has a mass flowrate range compatible with the chosen print speed, and can operate at 270 °C melt temperature [42] and has a power consumption range of 0.975–2.2 kW. Conservatively, using the upper limit for the power rating at the calculated time, the per part energy consumption for the BAAM printer is estimated to be 0.218 MJ.

3 Data and Results

Developed by the Environmental Protection Agency in the US, the TRACI 2.1 (Tool for the Reduction and Assessment of Chemical and other Environmental Impacts) methodology is used to calculate the environmental impacts for both inventories with the help of SimaPro [43]. TRACI 2.1 is a popular and well accepted impact assessment methodology within the LCA community, especially in the US.

Figure 3 shows a comparative graph between IM and AM magnet according to the TRACI methodology. The graph shows that across all impact categories, the AM magnets produce approximately 11% less impact compared to IM magnets across all environmental categories. This static constant difference between AM and IM magnets is due to the difference in their magnet powder consumption, which makes up 99.99% of the impact for both types of magnets. That is because the neodymium–iron–boron magnet powder inventory sourced from the excel tool provided by Arshi et al. [20] accounts for numerous energy intensive and environmentally polluting processes, in particular the electricity consumption for granulation of the powder and the mining and processing of the neodymium and dysprosium from China. The background data used to represent the LCI for Chinese electricity is modeled after the State Grid Corporation of China (SGCC) market, which generates 80% of its energy from fossil fuel sources, with 60% coming from coal and 20% energy sourced from oil-based plants [44]. With time, as China shifts towards cleaner sources of electricity, the environmental damage for producing permanent rare earth damage can be expected to decrease significantly. Hence, as AM magnets need

Table 7 LCI for injection molded magnet—tooling coating

Unit process	Amount	Unit	Source
Titanium powder	3.328×10^{-08}	kg	Titanium, primary {GLO}|market for|APOS, S
Silver	$4.44706\text{E} \times 10^{-13}$	kg	Silver {GLO}, market for|APOS,U
Polydimethylsiloxane	1.03765×10^{-12}	kg	Polydimethylsiloxane {GLO}|market for polydimethylsiloxane|APOS, S
Silica sand	1.48235×10^{-13}	kg	Silica sand {GLO}|market for|APOS, S
Silicon	1.48235×10^{-13}	kg	Silicon, electronics grade {GLO}|market for|APOS, S
Ethanol	0.0000016	kg	Ethanol, without water, in 99.7% solution state, from ethylene {RER}|market for ethanol, without water, in 99.7% solution state, from ethylene|APOS, S
Isopropanol	0.0000016	kg	Isopropanol {RER}|market for isopropanol|APOS, S
Aluminum oxide	1.04667×10^{-05}	kg	Aluminum oxide {GLO}|market for|APOS, S
De-ionized water	0.00007	kg	Water, de-ionized, from tap water, at user {GLO}|market for|APOS, S
Compressed air	1.06667×10^{-05}	m^3	Compressed air, 1000 kPa gauge {RER}|market for compressed air, 1000 kPa gauge|APOS, S
Powderization	9.73931×10^{-07}	MJ	Electricity, at grid, SERC, 2010/kWh/RNA
Apparatus cleaning	0.00000288	MJ	Electricity, at grid, SERC, 2010/kWh/RNA
Sandblasting	0.000079584	MJ	Electricity, at grid, SERC, 2010/kWh/RNA
Gas system	0.0000648	MJ	Electricity, at grid, SERC, 2010/kWh/RNA
Deposition process	0.001793376	MJ	Electricity, at grid, SERC, 2010/kWh/RNA

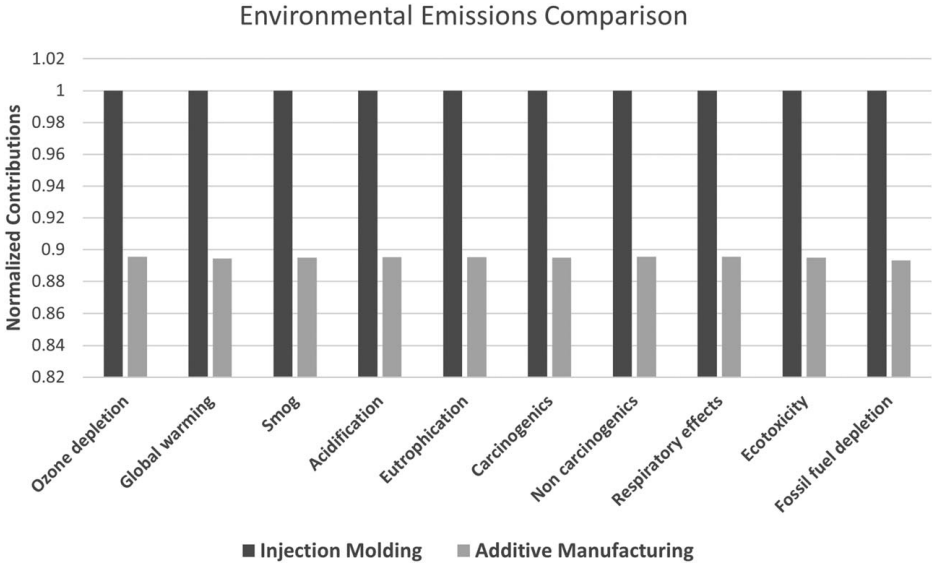

Fig. 3 Injection molding versus additive manufacturing environmental impact (TRACI)

11% less magnet powder by mass, they have around 11% less impact across all environmental categories.

Since sourcing of the rare earth magnetic powder appreciatively skews the date, it is important to consider the scenario when the powder blend is sourced from recycled magnets. Both AM and IM magnets can be recycled by cryomilling the original magnet into powder form, as demonstrated in Ref. [45]. Therefore, assuming the recycling of AM and IM magnets does not significantly differ in material or energy consumption, we can consider this scenario by neglecting the powder (both polymer and magnetic) inventories, along with the energy consumption for blending the powders in the pelletizing step (since the cryomilled powder will be already appropriately blended). Figure 4 shows the comparison between IM and AM magnets made from recycled materials.

In this scenario as well, the AM magnets are >20% better across all environmental categories. For the ozone depletion category, for example, the AM magnet has 30% of the impact as IM magnet. This is due to the tool coating within the IM inventory, as the aluminum oxide used has a high ozone depletion characterization factor.

4 Discussion

A large part of why AM magnets have a better environmental performance than IM magnets has to do with the loading ratio. Since they can accept a higher magnet powder by percentage, not only does it increase their energy product (as it is proportional to f^2) and result in a reduced required volume (and therefore mass) but also reduces amount of polymer binder used in the magnet. This is an important factor as the heating and melting of the polymer are more energy intensive than heating the magnet powder (as the polymer has four times the specific heat as the magnet powder and melting of the polymer requires overcoming the heat of fusion). Since all three processes—pelletization, IM, and AM—rely on heating and melting of the magnet–polymer mixture (in powder or pellet form), this results in an all-around effect of lower energy consumption for AM magnets. The low mass percentage of polymer in the mixture is also the reason why the total calculated energy consumption efficiencies of 0.467 and 0.335 MJ/kg for IM and AM, respectively, are drastically lower than reported efficiencies for purely plastic injection molding and additive manufacturing [46].

The results show that manufacturing magnets using BAAM printers have significant promise in becoming a more environmentally friendly alternative to injection molding. Recent progress shows that extrusion-based AM technology can support f as high as 75–80% [47]. This could significantly improve the $(BH)_{max}$, lower required bonded magnet volume and mass, and reduce the amount of consumption of critical rare earth magnetic material. The volume would decrease at around $1/f^2$ and the magnetic

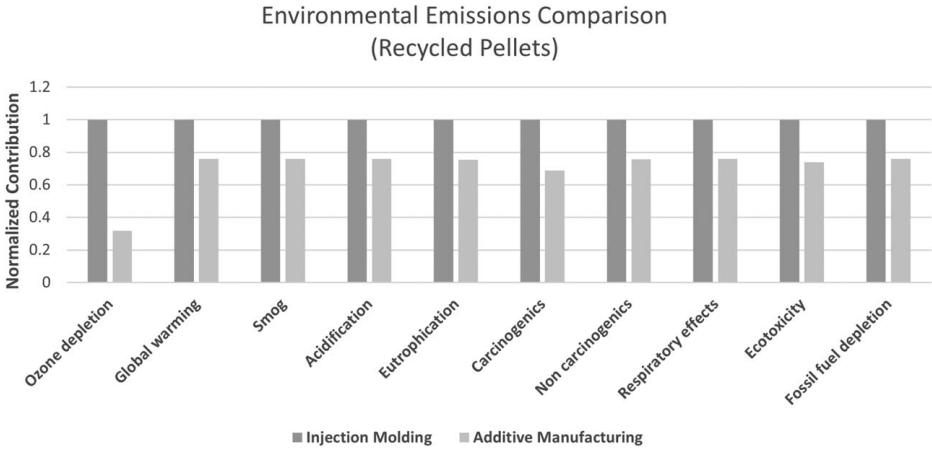

Fig. 4 Injection molding versus additive manufacturing (recycled pellets)—TRACI methodology

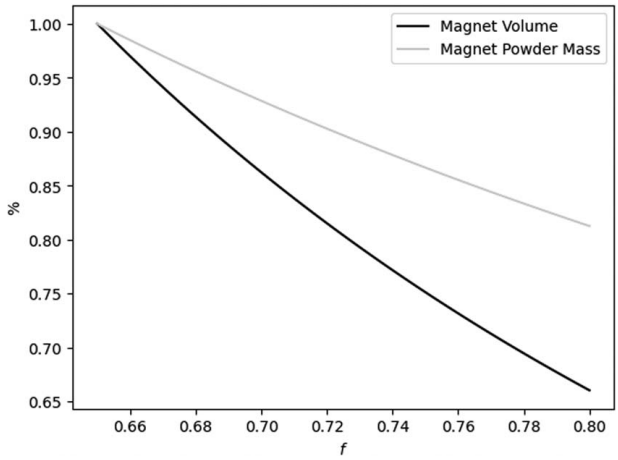

Fig. 5 Percent of original bonded volume magnet and magnetic material consumption (at $f = 65\%$) versus loading fraction

material consumption would decrease at around $1/f$. This relationship is shown in Fig. 5, where the percent magnet volume and percent magnet powder mass (of the original values at loading fraction of 65%) are shown as a function of the loading fraction.

BAAM printed magnets have other advantages over IM magnets that are not factored into the LCA. One such advantage is that BAAM printers have functionality that allows for composite printing [48]. Therefore, different pellet types can be used at different locations during printing. This allows for magnets to be printed that have magnetic powder concentrated where it is required and have more mechanical structure support where needed. This allows for creation of even more complex magnets and could drastically reduce the amount of required neodymium–iron–boron magnet powder without sacrificing performance. Furthermore, differences in transportation in the supply chain of these two manufacturing processes can be crucial depending on the application. Currently, injection molded magnets are manufactured at a central location and transported to the place of their usage. However, with BAAM printers, these magnets can also be manufactured directly at the location, requiring only the transportation of the pellets (which are much easier, and therefore much cheaper, to transport). These environmental and economic savings are more apparent for rare earth magnets used in windmills, which can weigh upwards of 1 ton [49] and need to be transported very carefully. The economic differences between additive manufacturing and injection molding go beyond transportation. The reduced consumption in magnetic powder for 3D printed magnets can result in huge savings as prices of rare earth minerals such as neodymium, dysprosium, or praseodymium have been increasing drastically due to the increasing demand [50]. Furthermore, the tooling process for injection molding is not only time consuming but also very expensive, as the mold has a large influence on the quality of the final product. Therefore, some preliminary economic assessment done by Post et al. show that the big area additive manufacturing process has the potential to be economically competitive [41]. However, a comprehensive techno-economic assessment (TEA) needs to be performed to evaluate for scalability, accounting for equipment, labor, transportation, and maintenance costs to make definitive claims regarding the economic performance of BAAM compared to injection molded magnets. The competitive advantage for BAAM can be magnified especially for permanent magnets that need to be customized and are produced at relatively smaller scales (injection molding is typically only profitable for scales greater than 20,000 parts or more [34]).

BAAM printers are still early in their adoption for large-scale manufacturing. However, these printers have already been commercialized, with several units already sold. Like IM magnets, work has already shown how motors designed to accept BAAM printed magnets with significantly lower eddy current losses due to high resistivity compared to sintered magnets. Hence, they have the potential to replace sintered magnets, in applications (e.g., motors) where these properties are desirable (assuming the magnetic performance is sufficient) [28]. However, we still do not know much about BAAM printers, such as their lifespan, how often does the extruder system need to be replaced, the extent of part geometry dependence for print speed, etc. The answer to these questions needs to be accounted within the LCA to get a more wholistic perspective on BAAM printers.

5 Conclusion

LCA results show that the novel magnets produced by the BAAM printers perform better than conventional injection molded magnets in terms of their environmental impacts. This improvement is largely due to BAAM's ability to accommodate higher loading fractions, resulting in 11% reduction of magnetic powder usage in the permanent magnet fabrication. However, as magnetic powder manufacturing is highly intensive, this represents almost all the savings in environmental impact. Since this reduction in magnetic powder usage has such drastic effects on the final environmental emissions, the LCA results suggest that future improvements in magnets produced via BAAM should focus on increasing the loading fraction. Furthermore, it is recommended that a full scale and thorough TEA be performed to see the feasibility of BAAM printed magnets against injection molded and sintered magnets. The TEA will also shed some more information on the potential adoption pathway for BAAM technology by the industry to print permanent bonded magnets.

Acknowledgment

This research was supported by the Critical Materials Institute, an Energy Innovation Hub funded by the U.S. Department of Energy, Office of Energy Efficiency and Renewable Energy, Advanced Manufacturing Office. Work was performed, in part, at Ames Laboratory operated for the U.S. Department of Energy by Iowa State University of Science and Technology under Contract No. DE-AC02-07CH11358. This manuscript has been authored in part by UT-Battelle, LLC, under contract DE-AC05-00OR22725 with the US Department of Energy (DOE). The US Government retains and the publisher, by accepting the article for publication, acknowledges that the US government retains a nonexclusive, paid-up, irrevocable, worldwide license to publish or reproduce the published form of this manuscript or allow others to do so, for US government purposes. DOE will provide public access to these results of federally sponsored research in accordance with the DOE Public Access Plan.[2]

Conflict of Interest

There are no conflicts of interest.

Data Availability Statement

The datasets generated and supporting the findings of this article are obtainable from the corresponding author upon reasonable request.

References

[1] Gutfleisch, O., Willard, M. A., Brück, E., Chen, C. H., Sankar, S. G., and Liu, J. P., 2011, "Magnetic Materials and Devices for the 21st Century: Stronger, Lighter, and More Energy Efficient," Adv. Mater., **23**(7), pp. 821–842.

[2] http://energy.gov/downloads/doe-public-access-plan

[2] DOE, "Critical Materials Rare Earths Supply Chain: A Situational White Paper 2020," https://www.energy.gov/sites/prod/files/2020/04/f73/Critical%20Materials%20Supply%20Chain%20White%20Paper%20April%202020.pdf, Accessed November 2, 2021.
[3] Yang, Y., Walton, A., Sheridan, R., Güth, K., Gauß, R., Gutfleisch, O., Buchert, M., et al., 2017, "REE Recovery From End-of-Life NdFeB Permanent Magnet Scrap: A Critical Review," J. Sustain. Metall., **3**(1), pp. 122–149.
[4] Alonso, E., Sherman, A. M., Wallington, T. J., Everson, M. P., Field, F. R., Roth, R., and Kirchain, R. E., 2012, "Evaluating Rare Earth Element Availability: A Case With Revolutionary Demand From Clean Technologies," Environ. Sci. Technol., **46**(6), pp. 3406–3414.
[5] Gambogi, J., "Rare Earths 2021," https://www.usgs.gov/centers/national-minerals-information-center/rare-earths-statistics-and-information, Accessed November 2, 2021.
[6] Nichols, R., "Final List of Critical Minerals 2018," Fed Regist 2018. https://www.federalregister.gov/documents/2018/05/18/2018-10667/final-list-of-critical-minerals-2018, Accessed October 11, 2021.
[7] Brown, D., Ma, B.-M., and Chen, Z., 2002, "Developments in the Processing and Properties of NdFeb-Type Permanent Magnets," J. Magn. Magn. Mater., **248**(3), pp. 432–440.
[8] Cui, J., Ormerod, J., Parker, D., Ott, R., Palasyuk, A., Mccall, S., Parans, M., et al., 2022, "Manufacturing Processes for Permanent Magnets: Part I—Sintering and Casting," JOM, **74**, pp. 1279–1295.
[9] Cui, J., Ormerod, J., Parker, D. S., Ott, R., Palasyuk, A., McCall, S., Parans, M., et al., 2022, "Manufacturing Processes for Permanent Magnets: Part II—Bonding and Emerging Methods," JOM, **74**, pp. 2492–2506.
[10] Ormerod, J., and Constantinides, S., 1997, "Bonded Permanent Magnets: Current Status and Future Opportunities," J. Appl. Phys., **81**(8), pp. 4816–4820.
[11] Wang, H., Lamichhane, T. N., and Paranthaman, M. P., 2022, "Review of Additive Manufacturing of Permanent Magnets for Electrical Machines: A Prospective on Wind Turbine," Mater. Today Phys., **24**, p. 100675.
[12] Li, L., Tirado, A., Nlebedim, I. C., Rios, O., Post, B., Kunc, V., Lowden, R. R., et al., 2016, "Big Area Additive Manufacturing of High Performance Bonded NdFeB Magnets," Sci. Rep., **6**(1), p. 36212.
[13] Li, L., Post, B., Kunc, V., Elliott, A. M., and Paranthaman, M. P., 2017, "Additive Manufacturing of Near-Net-Shape Bonded Magnets: Prospects and Challenges," Scr. Mater., **135**, pp. 100–104.
[14] Paranthaman, M. P., Yildirim, V., Lamichhane, T. N., Begley, B. A., Post, B. K., Hassen, A. A., Sales, B. C., Gandha, K., and Nlebedim, I. C., 2020, "Additive Manufacturing of Isotropic NdFeB PPS Bonded Permanent Magnets," Materials, **13**(15), p. 3319.
[15] Gutowski, T., Jiang, S., Cooper, D., Corman, G., Hausmann, M., Manson, J.-A., Schudeleit, T., et al., 2017, "Note on the Rate and Energy Efficiency Limits for Additive Manufacturing," J. Ind. Ecol., **21**(S1), pp. S69–79.
[16] Chesser, P., Post, B., Roschli, A., Carnal, C., Lind, R., Borish, M., and Love, L., 2019, "Extrusion Control for High Quality Printing on Big Area Additive Manufacturing (BAAM) Systems," Addit. Manuf., **28**, pp. 445–455. https://doi.org/10.1016/j.addma.2019.05.020.
[17] Sprecher, B., Xiao, Y., Walton, A., Speight, J., Harris, R., Kleijn, R., Visser, G., and Kramer, J., 2014, "Life Cycle Inventory of the Production of Rare Earths and the Subsequent Production of NdFeB Rare Earth Permanent Magnets," Environ. Sci. Technol., **48**(7), 3951–3958. https://doi.org/10.1021/es404596q
[18] Jin, H., Afiuny, P., McIntyre, T., Yih, Y., and Sutherland, J. W., 2016, "Comparative Life Cycle Assessment of NdFeB Magnets: Virgin Production Versus Magnet-to-Magnet Recycling," Proc. CIRP, **48**, pp. 45–50.
[19] Langkau, S., and Erdmann, M., 2021, "Environmental Impacts of the Future Supply of Rare Earths for Magnet Applications," J. Ind. Ecol., **25**(4), pp. 1034–1050.
[20] Arshi, P. S., Vahidi, E., and Zhao, F., 2018, "Behind the Scenes of Clean Energy: The Environmental Footprint of Rare Earth Products," ACS Sustain. Chem. Eng., **6**(3), pp. 3311–3320.
[21] ISO E. 14040:2006, "Environmental Management Life Cycle Assessment—Principles Framework." Eur. Comm. Stand. 2006.
[22] Coey, J. M. D., 2002, "Permanent Magnet Applications," J. Magn. Magn. Mater., **248**(3), pp. 441–456.
[23] Ireland, J. R., 1967, "New Figure of Merit for Ceramic Permanent Magnet Material Intended for DC Motor Applications," J. Appl. Phys., **38**(3), pp. 1011–1012.
[24] Binns, K. J., and Shimmin, D. W., 1996, "Relationship Between Rated Torque and Size of Permanent Magnet Machines," IEE Proc. Electr. Power Appl., **143**(24), pp. 417–422.
[25] Ma, B. M., Herchenroeder, J. W., Smith, B., Suda, M., Brown, D. N., and Chen, Z., 2002, "Recent Development in Bonded NdFeB Magnets," J. Magn. Magn. Mater., **239**(1–3), pp. 418–423.
[26] Garrell, M. G., Shih, A. J., Ma, B.-M., Lara-Curzio, E., and Scattergood, R. O., 2003, "Mechanical Properties of Nylon Bonded Nd–Fe–B Permanent Magnets," J. Magn. Magn. Mater., **257**(7), pp. 32–43.
[27] Gandha, K., Nlebedim, I. C., Kunc, V., Lara-Curzio, E., Fredette, R., and Paranthaman, M. P., 2020, "Additive Manufacturing of Highly Dense Anisotropic Nd–Fe–B Bonded Magnets," Scr. Mater., **183**, pp. 91–95.
[28] Li, L., Jones, K., Sales, B., Pries, J. L., Nlebedim, I. C., Jin, K., Bei, H., et al., 2018, "Fabrication of Highly Dense Isotropic Nd–Fe–B Nylon Bonded Magnets Via Extrusion-Based Additive Manufacturing," Addit. Manuf., **21**, pp. 495–500. https://doi.org/10.1016/j.addma.2018.04.001
[29] Polyamide 6—Nylon 6—PA 6, "AZoMCom 2001." https://www.azom.com/article.aspx?ArticleID=442, Accessed November 2, 2021.
[30] Wernet, G., Bauer, C., Steubing, B., Reinhard, J., Moreno-Ruiz, E., and Weidema, B., 2016, "The Ecoinvent Database Version 3 (Part I): Overview and Methodology," Int. J. Life Cycle Assess., **21**(9), pp. 1218–1230.
[31] Piccinno, F., Hischier, R., Seeger, S., and Som, C., 2016, "From Laboratory to Industrial Scale: A Scale-Up Framework for Chemical Processes in Life Cycle Assessment Studies," J. Clean. Prod., **135**, pp. 1085–1097.
[32] Liang, M., Huff, H. E., and Hsieh, F.-H., 2002, "Evaluating Energy Consumption and Efficiency of a Twin-Screw Extruder," J. Food Sci., **67**(5), pp. 1803–1807.
[33] Rauwendaal, C., 2014, "10—Twin Screw Extruders," *Polymer Extrusion*, 5th ed., C. Rauwendaal, ed., Hanser, pp. 697–761. https://doi.org/10.3139/9781569905395.010
[34] Merhar, J. R., 1990, "Overview of Metal Injection Moulding," Met. Powder Rep., **45**(5), pp. 339–342.
[35] Raoufi, K., Harper, D. S., and Haapala, K. R., 2020, "Reusable Unit Process Life Cycle Inventory for Manufacturing: Metal Injection Molding," Prod. Eng., **14**(5–6), pp. 707–716.
[36] Specific Heat of some common Substances, n.d., https://www.engineeringtoolbox.com/specific-heat-capacity-d_391.html, Accessed November 2, 2021.
[37] Fiameni, S., Battiston, S., Castellani, V., Barison, S., and Armelao, L., 2021, "Implementing Sustainability in Laboratory Activities: A Case Study on Aluminum Titanium Nitride Based Thin Film Magnetron Sputtering Deposition Onto Commercial Laminated Steel," J. Clean. Prod., **285**, p. 124869.
[38] Peng, T., and Sun, W., 2017, "Energy Modelling for FDM 3D Printing From a Life Cycle Perspective," Int. J. Manuf. Res., **12**(1), pp. 83–98.
[39] Jiang, S., 2017, "Processing Rate and Energy Consumption Analysis for Additive Manufacturing Processes: Material Extrusion and Powder Bed Fusion," Thesis, Massachusetts Institute of Technology, Cambridge, MA.
[40] Roschli, A. C., 2016, "Dynamic Extruder Control for Polymer Printing in Big Area," Addit. Manuf.
[41] Post, B. K., Lind, R. F., Lloyd, P. D., Kunc, V., Linhal, J. M., and Love, L. J., 2016, "The Economics of Big Area Additive Manufacturing," 2016 International Solid Freeform Fabrication Symposium, Austin, TX, Aug. 8–10, University of Texas at Austin.
[42] Gigabot X XLT—re:3D|Life-Sized Affordable 3D Printing, n.d., https://re3d.org/portfolio/gigabot-x-xlt/, Accessed October 8, 2021.
[43] Bare, J., 2011, "TRACI 2.0: The Tool for the Reduction and Assessment of Chemical and Other Environmental Impacts 2.0," Clean Technol. Environ. Policy, **13**(5), pp. 687–696.
[44] IEA, 2021, *An Energy Sector Roadmap to Carbon Neutrality in China*, IEA, Paris.
[45] Gandha, K., Ouyang, G., Gupta, S., Kunc, V., Parans Paranthaman, M., and Nlebedim, I. C., 2019, "Recycling of Additively Printed Rare-Earth Bonded Magnets," Waste Manage., **90**, pp. 94–99.
[46] Thiriez, A., and Gutowski, T., 2006, "An Environmental Analysis of Injection Molding," Proceedings of the 2006 IEEE International Symposium on Electronics and the Environment 2006, Scottsdale, AZ, May 8–11, pp. 195–200.
[47] Paranthaman, M. P., Cramer, C. L., Nandwana, P., Elliott, A. M., and Chinnasamy, C., 2021, "Indirect Additive Manufacturing Process for Fabricating Bonded Soft Magnets."
[48] Duty, C. E., Kunc, V., Compton, B., Post, B., Erdman, D., Smith, R., Lind, R., Lloyd, P., and Love, L., 2017, "Structure and Mechanical Behavior of Big Area Additive Manufacturing (BAAM) Materials," Rapid Prototyp. J., **23**(1), pp. 181–189.
[49] Jacoby, M., and Jiang, J., 2010, "Securing the Supply of Rare Earths," Chemical and Engineering News. https://cen.acs.org/articles/88/i35/Securing-Supply-Rare-Earths.html, Accessed November 2, 2021.
[50] "Boom, Bust and Boom Again for Rare Earths?" Reuters 2017, https://www.reuters.com/article/us-china-rareearths-ahome-idUSKCN1BC4OF, Accessed November 2, 2021.